Ground Support 2023 – J Wesseloo (ed.)

doi:10.36487/ACG_repo/2325_12

Utilisation of seismic data in the assessment of displacement and energy demand imposed on ground support by strainbursts

D Malovichko *Institute of Mine Seismology, Australia*

Abstract

Conventional processing of seismic monitoring data recorded in mines often adopts models and methods established in global seismology and focused mainly on tectonic earthquakes. These models and methods make it possible to evaluate geometrical and mechanical characteristics of sources (e.g. orientation and dimensions of the slip surface or shear failure zone, the direction and amount of slip or shear deformation) and the intensity of associated ground motion (typically, peak ground velocity in the vicinity of failure and at a distance from it). Forecasting of ground motion intensity for planned mining is important for the assessment of energy demand on ground support in terms of shakedown damage. Strong ground motion temporarily increases stress around tunnels and may also deepen the depth of failure, which will cause dynamic loading of ground support due to bulking (induced strainbursting damage mechanism).

A new seismic source model has been suggested in recent years. It describes seismic radiation from an episode of sudden stress fracturing around a tunnel. The model makes it possible to infer the increment in the depth of failure and duration of this process from recorded seismic signals. Application of this model to relevant seismic events (those locating to tunnels with crush-type mechanisms) can be used to: (a) establish a relation between bulking duration and increment in the depth of failure (depth of strainbursting), (b) evaluate the cumulative depth of strainbursting for tunnels of the mine, (c) assess the amount and probability of strainbursting realisations. The paper discusses these applications and their utilisation for the assessment of displacement and energy demand on ground support.

Keywords*: crush-type seismic source mechanism, depth of strainbursting, bulking duration*

1 Introduction

The source of a tectonic earthquake is the shear fracture of the earth's material along a (plane) surface, which is initiated over a small area and then propagates at a velocity not exceeding the velocity of P-waves (modified from Kostrov & Das 1988). The seismic radiation far away from such a source (i.e. at distances much larger than the dimensions of the fracture zone) can be described by a conventional double-couple model. This means that the radiation can be modelled by the two-step procedure: (1) removing the fracturing rock from the medium (i.e. 'backfilling' it with elastic material); and (2) applying two fictitious force couples with zero net moment at the location of fracture.

The parameters of double-couple model evaluated from the seismic waveforms of tectonic earthquakes are useful for the analysis of their sources. For example, the directions of the couples provide possible orientation of shear fracture surface and direction of shearing. The magnitudes of the couples (scalar seismic moment) correspond to the product of shear fracture area, average displacement across it and shear modulus of the medium surrounding the fracture.

Various models and empirical relations were suggested for the assessment of characteristics of fracture at the source and associated ground motion:

- Source size: radius of circular fault from a corner frequency (Brune 1970; Madariaga 1976; Brune et al. 1979).

- Stress release: static stress drop (Brune 1970), dynamic stress drop (Boatwright 1980).
- Displacement at the source: average slip from seismic moment (Somerville et al. 1999).
- Near-source ground motion: near-fault peak ground velocity (McGarr 1991).

The list above is not comprehensive. It serves to illustrate the variety of approaches available for analysis of seismic sources which correspond to a double-couple point source model.

The principal hazard of tectonic earthquakes is related to strong ground motion (ground shaking). For example, a study of damage to buildings associated with 50 earthquakes (Bird & Bommer 2004) shows that ground shaking was the primary cause of damage in 88% of cases. Landslides, tsunamis, liquefaction and fault rupture were the primary cause of damage in the remaining 12% of cases or played a secondary role. Correspondingly, one of the main focuses of earthquake engineering is to forecast the intensity of ground shaking (accounting for source characteristics, distance and amplification in superficial geological layers) and quantify the likelihood of damage to a particular type of structure (building, bridge etc.).

The aforementioned seismic source model and methods of analysis of seismic data are used widely in mine seismology. Seismic events recorded in mines are often interpreted using the source models of tectonic earthquakes and corresponding parameters are reported (e.g. radius of circular fault, static stress drop and nodal planes). Similar to earthquake engineering, the dynamic loading to mine tunnels is often evaluated in terms of intensity of ground motion (e.g. using peak ground velocity). The latter is important for the assessment of energy demand on ground support in terms of shakedown damage (left of Figure 1). Strong ground motion temporarily increases stress around tunnels and may also deepen the depth of failure, which will cause dynamic loading of ground support due to bulking (induced strainbursting damage mechanism). Various aspects of demand imposed on ground support in terms of ground motion were discussed in publications (Kaiser et al. 1996; Potvin & Wesseloo 2013; Mendecki 2016; Morissette & Hadjigeorgiou 2019; Malovichko & Kaiser 2020; Kaiser & Moss 2022; and many others) and will not be covered in this paper.

It is important to keep in mind that the source model of a tectonic earthquake cannot be universally applied to seismic data recorded at mines. There are, at least, two reasons for this:

- Dynamic fracture processes in mines are not always localised within a narrow zone, which can be approximated by (plane) surface. For example, fracturing often happens near the perimeter of excavations (tunnels, stopes, caves), and the surrounding rock mass experiences convergence during the fracturing. Other examples include failures driven by gravity such as rockfalls, episodes of sudden movement of rocks in stopes or caves, or landsliding in the hanging wall of inclined mined-out ore bodies. Various sources of seismic events observed in mines are discussed by Hasegawa et al. (1989).
- Seismic radiation for events induced by mining can often not be explained by a double-couple model. For example, there were multiple reports about implosive source mechanisms, implying that seismic sensors experience first motion predominantly oriented towards the source (McGarr 1992; Stickney & Sprenke 1993; Julia et al. 2009).

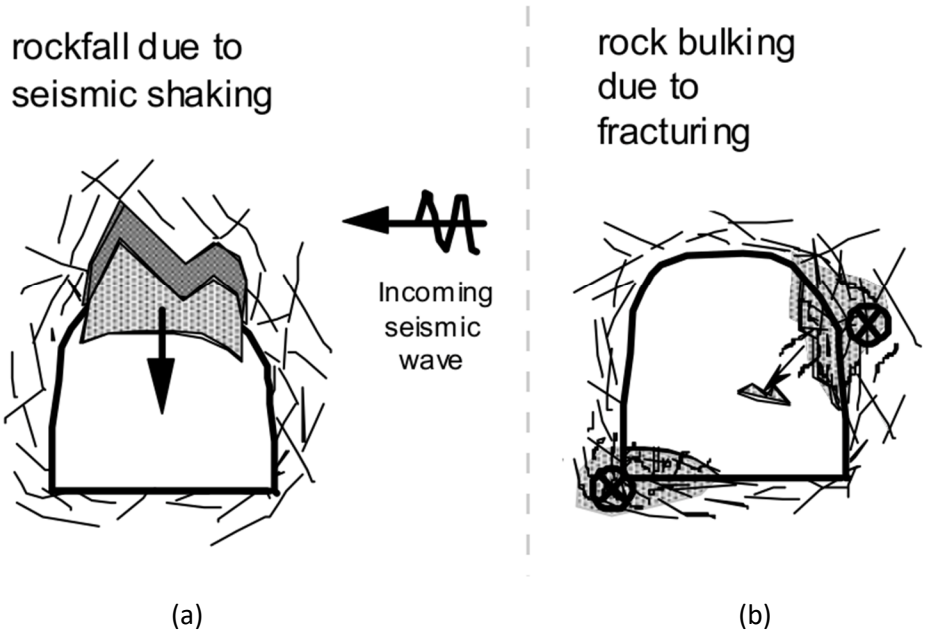

Figure 1 Two types of rockbursts described in Kaiser & Moss (2022) based on Kaiser et al. (1996): (a) Shakedown, which causes damage to an excavation or its support by a seismically induced fall of ground; (b) Strainburst, which is an excavation or support failure process whereby a highly stressed volume of unsupported or supported rock bursts near an excavation

The main focus of this paper is on the process of sudden stress fracturing around excavation (right of Figure 1) and its associated seismic radiation (i.e. when the excavation failure process is part of the seismic source). These are illustrated in Figure 2, which represents modelling Case 3 as performed by Malovichko & Rigby (2022). Note that the shown failure process is not caused or triggered by seismic waves from an external seismic source. It is quite the opposite: the failure and associated deformation of the rock mass around a tunnel radiate seismic waves and, therefore, represent a seismic source. The radiated seismic waves are not the cause of rock fracturing; rather they are merely a byproduct of it. Correspondingly, the intensity of seismic radiation (expressed in terms of peak ground velocity or other ground motion parameters) may be insufficient on its own to describe the dynamic demand on ground support. The preferred approach, as discussed in this paper, is to use the characteristics of seismic radiation to assess the amount and rate of the stress fracturing and, consequently, translate these to parameters describing displacement and energy demand.

The current paper presents the models and methods discussed in Kaiser & Malovichko (2022), Malovichko & Rigby (2022), and Malovichko (2022), and extends some aspects of these. Section 2 briefly overviews a seismic source model of self-initiated or triggered strainbursting around a tunnel, along with the procedures of seismological assessment of the depth of strainbursting and bulking duration. Section 3 shows how the cumulative depth of strainbursting can be evaluated from seismic data. Strainbursting hazard (amount and likelihood of strainburst realisation) is considered in Section 4. The incorporation of seismic data into the deformation-based support design (DBSD) methodology of Kaiser & Moss (2022) is covered in Section 5. The recommendation of seismic data utilisation in the forensic assessment of dynamic demand imposed on ground support in cases of rockburst damage are provided in the Conclusion, together with suggestions for further work.

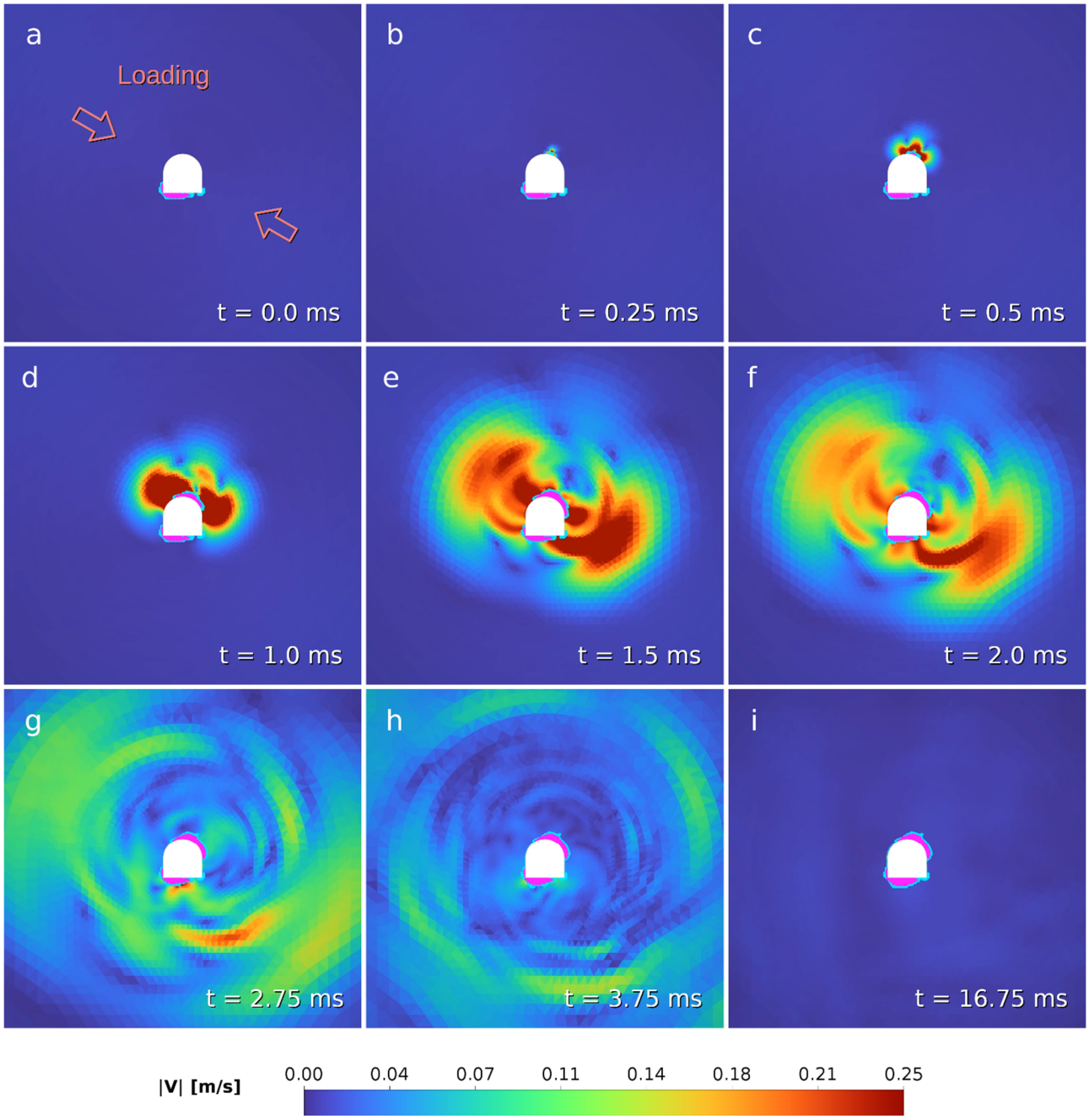

Figure 2 **Modelling of dynamic stress fracturing on the perimeter of a tunnel (Malovichko & Rigby 2022). The tunnel is loaded by maximum principal stress plunging from the top left corner to the bottom right corner. Magenta and cyan colours indicate the zones of failure with tensile and compressive volumetric strain, respectively. The background colour ranging from blue to red describes the absolute amplitude of ground velocity. In the original state (a) failure zone is localised to the floor and bottom left corner. Slow loading of the tunnel causes spontaneous nucleation of the failure between the back and right shoulder (b), which dynamically evolves, radiating seismic waves (c–h). Dynamic growth of the failure zone also happens in the bottom left corner (g–h), which further contributes to seismic radiation. Finally the rock mass around the tunnel settles in a stable state (i)**

2 Relation between bulking duration and depth of strainbursting

Figure 2 clearly shows that spontaneous stress fracturing around a tunnel radiates seismic waves. The illustrated radiation is represented by high-frequency waves (with the wavelengths in the order of 1 m), which are typically not recorded by mine-wide seismic systems with distances between seismic sensors in the order of several hundred metres. The seismic systems of mines usually provide data suitable for analysis of source mechanisms (including scalar seismic moment) at much lower frequencies, i.e. wavelengths in the order of tens or hundreds of metres. The process demonstrated in Figure 2 also produces radiation at such low frequencies that it is not visible in the images. The high-frequency radiation (which is typically not recorded) contains information about the details of the fracturing process (e.g. initiation of failure in the shoulder and its later evolution in the bottom corner as shown in Figure 2). The low-frequency radiation does not capture all these details, and it is mainly controlled by the overall deformation of rock mass around the tunnel between the initial (Figure 2a) and final (Figure 2i) states. It is expected that this deformation generally corresponds to the convergence of the rock mass towards the tunnel.

The characteristics of the low-frequency part of seismic radiation associated with stress fracturing around a single tunnel were studied by Malovichko & Rigby (2022). It was shown that this radiation can be modelled by the process of growth of elliptical cavity in elastic medium (Figure 3). The geometrical parameters of the model shown in Figure 3 were used to describe the seismic source mechanism. The mechanisms obtained for different modelled variants of failure around tunnels had common features: significant implosive component and pancake-shape deviatoric component, which together correspond to a closing crack model. The P-axis of mechanisms correlated with the direction of loading (marked in Figure 3). Following the terminology of Ryder (1988), it was suggested the mechanisms possessing these features be named as ‘crush-type’.

The scalar seismic moment corresponding to a crush-type mechanism associated with a tunnel can be approximated as:

$$|M| \approx 2\frac{1-\nu}{1-2\nu}|\sigma_{max}|L_A\left(D+\frac{1}{2}\Delta d_f\right)\Delta d_f, \quad (1)$$

where:

ν	=	Poisson’s ratio for the rock mass.
$\lvert\sigma_{max}\rvert$	=	maximum far-field principal stresses orthogonal to the tunnel’s axis.
$\Delta d_f = \Delta d_f^1 + \Delta d_f^2$	=	increase in depth of failure in the direction of minimum far-field principal stresses orthogonal to the tunnel’s axis.
$D+\frac{1}{2}\Delta d_f$	=	effective tunnel dimension in that direction.
L_A	=	length of dynamic fracturing along the tunnel.

Equation 1 can be used to evaluate the increment in the depth of failure, which is called the depth of strainbursting, d_{SB}, by Kaiser & Malovichko (2022), as this increment happens in a dynamic form (i.e. accompanied by the radiation of seismic waves). A simple approach is to assume that the distribution of Δd_f along the tunnel is uniform. However, it is considered more realistic to have the largest increment in the depth of failure at a local part of the tunnel, with a gradual decrease to zero increment in both directions along the tunnel. In particular, assuming:

1. A cosine shape of Δd_f distribution along the tunnel with the peak value Δd_f^{max}, and
2. A fixed ratio of Δd_f^{max} and L_3: $R = \Delta\, d_f^{max}/L_A$,

the depth of strainbursting can be evaluated as:

$$d_{SB} = \Delta d_f^{max} \approx d_0 + d_e, \quad (2)$$

where:

$$d_0 = \sqrt{\pi |M| R\,(1-2\nu)/[4(1-\nu)|\sigma_{max}|D]}$$

$$d_e = -d_0^2/(3d_0 + 16\,D/\pi)$$

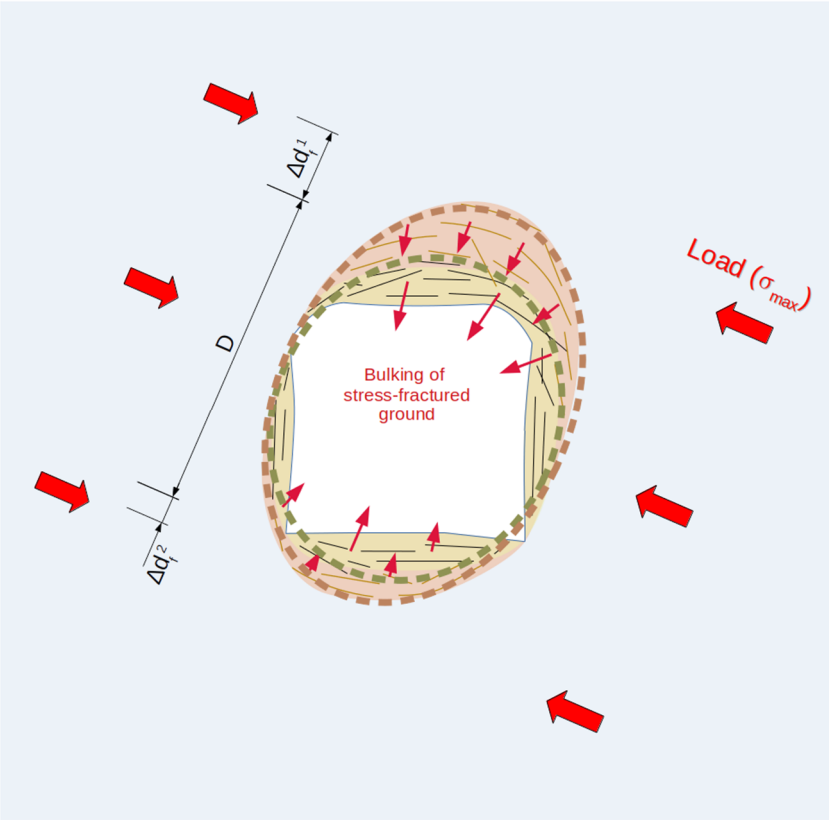

Figure 3 View looking along a tunnel showing failed rock before (yellow) and after (red) a strainburst. The dashed contours represent the approximation of a tunnel and its damage zone by pre- and post-strainburst elliptical cavities. The labelled geometrical parameters of the cavities are used in the expression for scalar seismic moment (described in the text)

Equation 1 and Figure 3 show that seismic moment combines the effect of failure across opposite sides of the tunnel. Crush-type seismic source mechanisms do not contain information on whether failure happened on one side of the tunnel (e.g. back only) or on both sides of it (e.g. back and floor). The split of failure between the sides needs to be established based on underground observations. In this paper we use a conservative assumption that stress fracturing happens on one side of the tunnel (e.g. either $\Delta d_f^1 = 0$ or $\Delta d_f^2 = 0$ in Figure 3). If the underground observations in a particular case suggest that strainbursting typically involves both opposite sides in an equal manner (i.e. $\Delta d_f^1 \approx \Delta d_f^2$), then the calculated values of d_{SB} can be halved.

As will be discussed in Section 5, the energy demand on ground support during strainbursting is defined by not only the amount of stress fracturing (quantified using d_{SB} and bulking factor), but also by the duration of this process. If we assume that fracturing and bulking of rock during strainburst is contained (i.e. the bulking rock remains mechanically coupled with the surrounding rock mass), then the duration of seismic radiation and duration of bulking will be approximately the same. Consequently, the measured seismic source duration provides an estimate of bulking duration, t_B.

It may be considered that t_B can be approximated by the inverse of corner frequency, traditionally estimated from the intersection of low- and high-frequency trends of source spectra. This approach may produce incorrect results as the traditional corner frequency is sensitive to small-scale episodes in the rupture history

of the source (Silver 1983) and does not necessarily characterise the overall duration and extent of the source.

The suggested approach (Malovichko 2022) is to calculate half duration of the source, DT_0, which is the time difference between centroid time evaluated from moment tensor inversion, T_0, and origin time calculated from the first arrivals of P- and S-waves, t_0 (Dziewonski & Woodhouse 1983): $DT_0 = T_0 - t_0$. The procedure is schematically illustrated in Figure 4. The bulking duration is $t_B = 2DT_0$.

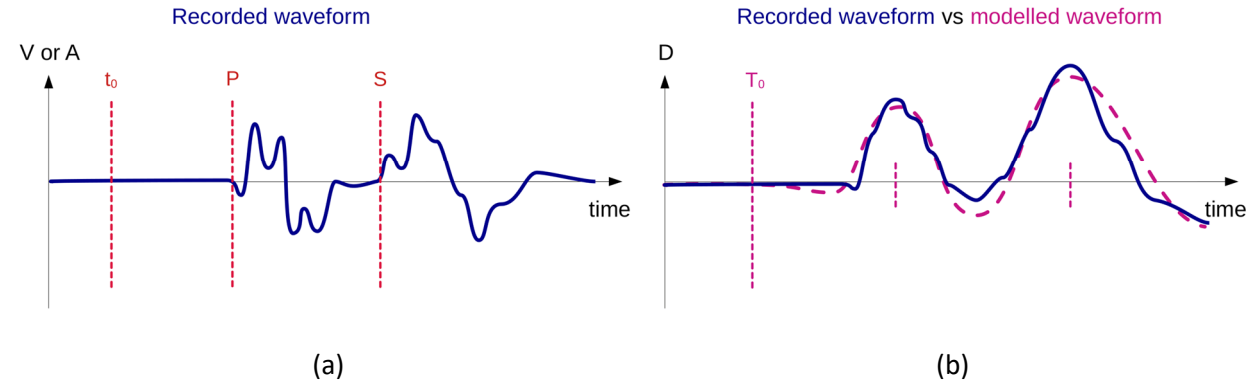

Figure 4 Schematic explanation of source duration assessment procedure. (a) The first arrivals of P- and S-waves are typically picked at velocity or acceleration waveforms and used to evaluate origin time, t_0, corresponding to the failure initiation; (b) Source mechanism inversion by matching filtered displacement waveforms provides an estimate of the centroid time, T_0, which corresponds to the temporal midpoint of source evolution

Examples of the assessment of d_{SB} and t_B using seismic data from six mines are presented in Figure 5. For all mines (except Mine B) the bulking duration ranges between 10 and 30 ms for typical depth of strainbursting between 0.1 and 1 m. For Mine B stress fracturing happens in a faster manner and energy demand on ground support is larger compared to other presented mines (for the same amount of stress fracturing quantified using d_{SB}). There is an overall tendency of t_B increase as d_{SB} grows.

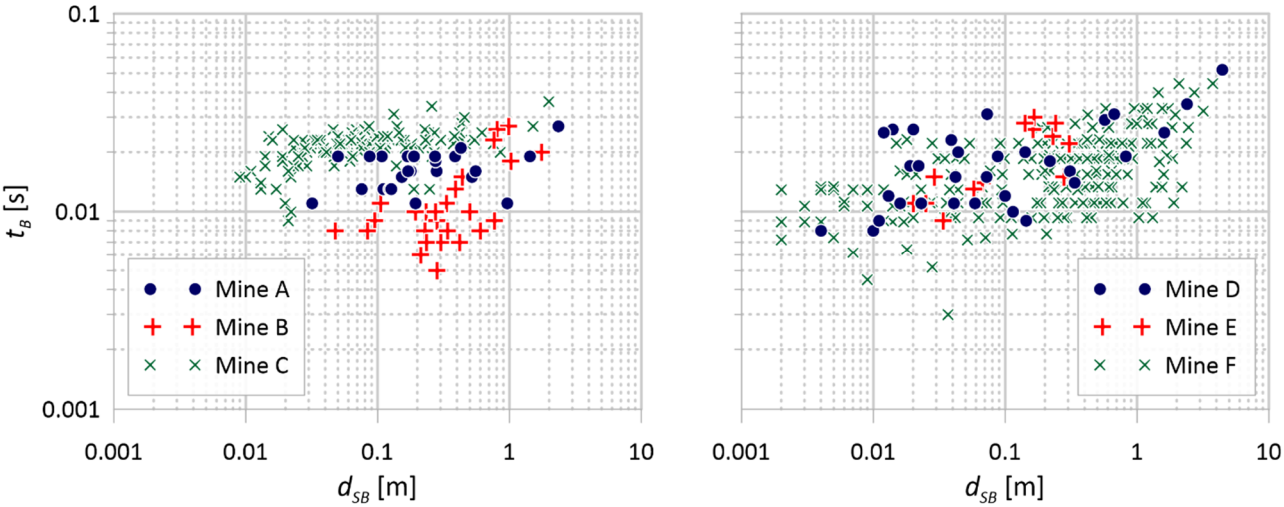

Figure 5 Parameters of strainbursting demand evaluated from seismic data: bulking duration t_B versus depth of strainbursting d_{SB}. Each data point represents a single crush-type event attributed to a tunnel

3 Cumulative depth of strainbursting

For each crush-type event associated with a tunnel it is possible to evaluate the depth of strainbursting, d_{SB}, and map it to the tunnel. This can be repeated for multiple crush-type events, providing the map of cumulative depth of strainbursting Σd_{SB}.

This procedure has a flaw: not all events have a source mechanism evaluated. Some of the events without mechanisms may correspond to sudden stress fracturing around tunnels and their contribution to Σd_{SB} will be missing if only events with mechanisms are used in the mapping. As an example, the top of Figure 6 shows seismic data from a mine. Some of the source mechanisms are of slip-type and they cannot be used in the Σd_{SB} mapping. The source mechanisms of events shown as blue spheres are not known and, therefore, it is unclear whether they can or cannot be used in the cumulation of the depth of strainbursting.

This problem can be addressed by converting seismic data to co-seismic strain using the gridding procedure described in Malovichko (2022). The procedure is illustrated in the middle of Figure 6. Each grid point contains the following parameters of strain:

- Cumulative moment (shown using contours).
- Orientations of maximum (compressional) and minimum principal strains (red and blue dipoles, respectively).
- Type of deformation (implosive – white sphere with red dipole, explosive – black sphere with blue dipole, deviatoric – dipoles).

It must be emphasised that events without source mechanisms contribute to the cumulative moment of grid points. The type of deformation in each grid point is defined by the average of normalised contributing mechanisms. The gridding procedure presumes that the type of deformation for each grid point remains the same for the time period represented by gridded seismic events.

Grid points neighbouring to tunnels with implosive co-seismic strain are used to evaluate Σd_{SB}. The resulting map for the considered example is shown in the bottom of Figure 6.

The described mapping procedure provides information not only about the amount of stress fracturing but also about its location along the perimeter of tunnels (i.e. whether it should be attributed to back, shoulders or sidewalls). For example, if the maximum (compressional) principal co-seismic strain is oriented horizontally and orthogonal to the tunnel direction, then it is expected that the stress-fractured volume evolved in the back and/or floor (which can be seen in Figure 6). If the maximum principal co-seismic strain is oriented vertically, then stress fracturing is expected in the sidewalls.

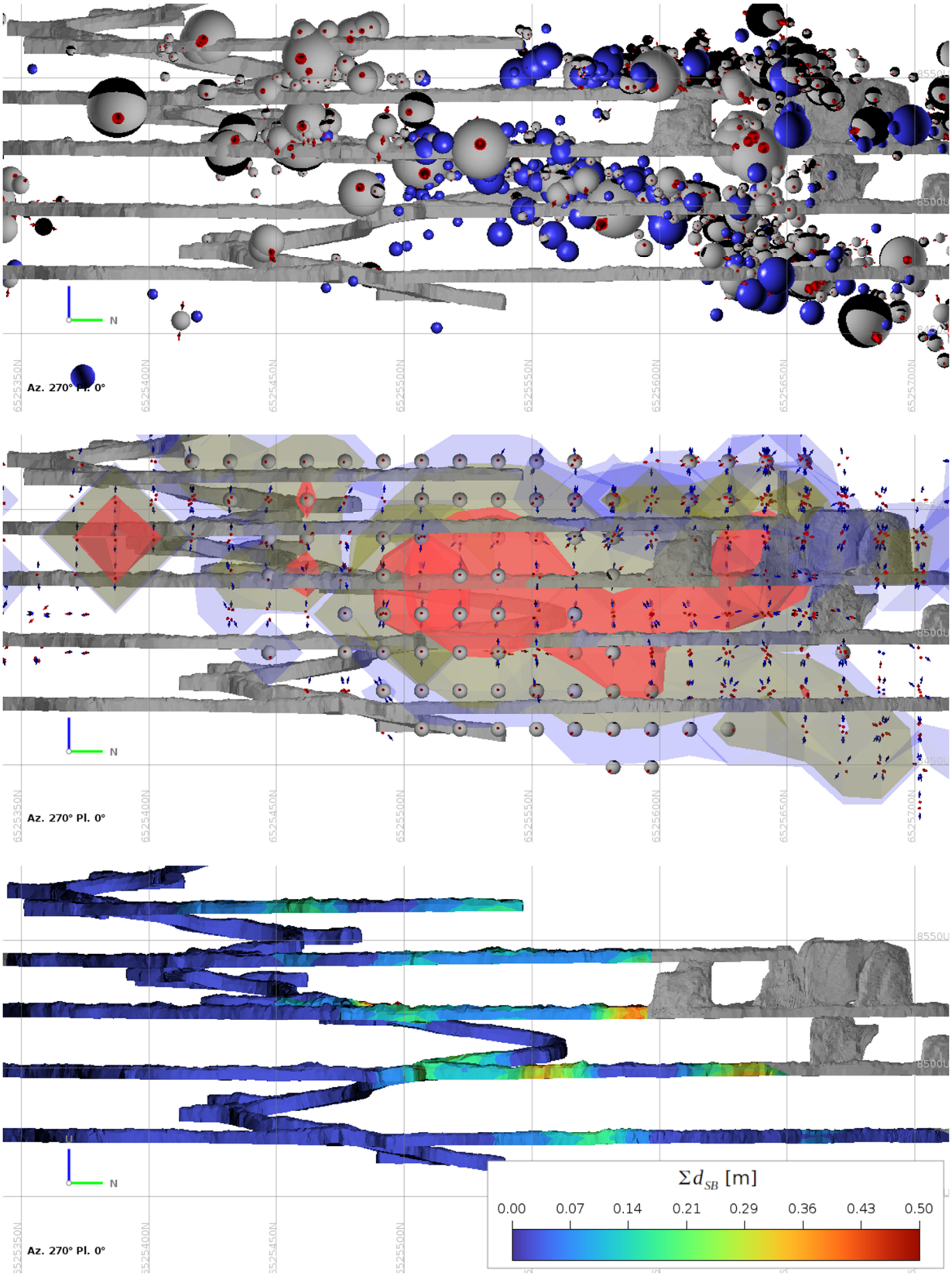

Figure 6 **Mapping of cumulative depth of strainbursting. Top: Seismic events are presented using beachballs with P-axes if source mechanism is available and as spheres if there the mechanism is unknown. Middle: Co-seismic strain field inferred from the presented events (see details in the text). Bottom: map of cumulative depth of strainbursting inferred from co-seismic strain**

4 Amount and probability of strainbursting realisation

The expected amount of stress fracturing around a tunnel can be modelled by taking the rock mass properties, stress field and geometrical characteristics of the tunnel and nearby excavations into account. The expression for extreme depth of failure, d_f^e, based on a stress level index (ratio of maximum tangential stress and uniaxial compressive strength) was suggested by Kaiser et al. (1996)[1]. Only a fraction of the modelled depth of failure may happen in dynamic form (as a strainburst) and, for the assessment of dynamic loading on ground support, it is important to quantify that fraction. Another limitation of the modelling is that it typically does not provide the probability of strainburst realisation (e.g. substantial depth of failure can be predicted by modelling for many tunnels, but strainbursting will happen only in a few of these). Seismic data can help to answer two questions:

- What percentage of the extreme depth of failure does typically happen in a dynamic form? Assuming that the percentage does not depend on the amount of stress fracturing, it can be expressed by a constant parameter q_{SB} as follows: $d_{SB} = q_{SB} d_f^e$.
- How often is the modelled depth of failure increase materialised in dynamic form? For example, if a section of tunnel of unit length (e.g. 5 m) remains in the same conditions (the expected extreme depth of failure d_f^e does not change) during a one-year period, then it is desirable to evaluate the (annual) probability of realisation, APE_{SB}, of a given depth of strainbursting, d_{SB}.

A crush-type event located in a tunnel with a modelled extreme depth of failure, d_f^e, provides an indication that a part of (or whole) expected depth of failure is materialised in dynamic form. This is the key idea behind the assessment of parameters q_{SB} and APE_{SB} from seismic data.

An approach to assess q_{SB} and APE_{SB} is illustrated in Figure 7 using data from a real block cave mine. The network of tunnels is approximated by nodes, with each node describing a five-metre tunnel section. The nodes are coloured according to the modelled extreme depths of failure, d_f^e, for three consecutive time periods, ΔT. The d_f^e change over time as the growing cave modifies the stress field. The crush-type events attributed to the tunnels and recorded during the selected time periods are shown as beachballs. There is a general tendency for the events to be clustered in the areas with the higher d_f^e. The cumulative depth of strainbursting, Σd_{SB}, can be assessed for each tunnel node and each time interval using the procedure described in Section 3.

It is suggested that the following expression be used to describe the probability of strainbursting realisation with a cumulative depth of failure increase of at least Σd_{SB} during the time period ΔT for a representative section of tunnel (e.g. of 5 m length), for which the modelling predicts the extreme depth of failure of d_f^e:

$$Pr\left(\Sigma d_{SB} | d_f^e = x\right) = PE_{SB} \Phi(ln\,(x\, q_{SB}/\Sigma\, d_{SB})/\beta) \quad (3)$$

where:

Φ = standard normal cumulative distribution function.

β = standard deviation.

The selection of this particular functional form is motivated by the framework of fragility functions adopted in earthquake engineering (Baker 2015). The probability of exceedance, PE_{SB}, for time period ΔT can be transformed to the annual probability of exceedance: $APE_{SB} = 1 - (1 - PE_{SB})^{1/\Delta T}$, where ΔT is expressed in years.

The assessment of parameters PE_{SB}, q_{SB} and β can be done using multiple stripes analysis proposed by Baker (2015). The following results were obtained for the case shown in Figure 7: q_{SB} = 0.24, β = 0.93 and

1 Note that d_f^e represents the deepest anticipated depth of failure along a tunnel. The mean depth is much less.

PE_{SB} = 0.104. This means that approximately a quarter of modelled extreme depth of failure is materialised in dynamic form, and the probability that it happens during time period ΔT is 10.4%.

The fit of data by the model (Figure 7d) is far from perfect. The improvement of the fit is within the domain of responsibility of stress modelling (provided that the seismic data is of high quality). In the ideal case the model will predict high values of extreme depth of failure in the areas and time periods where crush-type events are recorded. By contrast there should be no crush-type events in the areas and time periods for which the modelled extreme depth of failure is low.

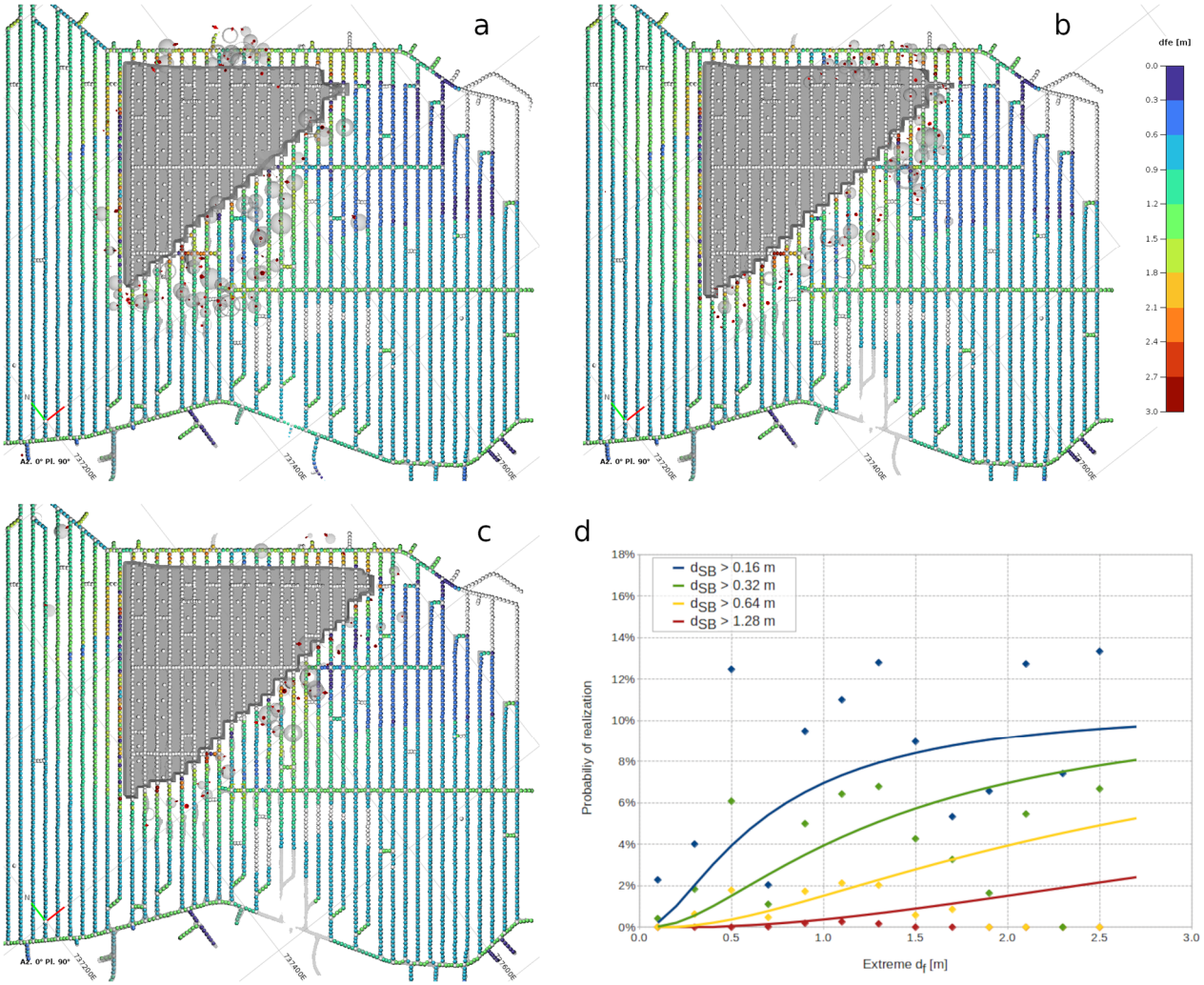

Figure 7 **(a–c) Maps of extreme depth of failure evaluated based on stress modelling and rock mass properties for three consecutive time periods. The recorded crush-type events associated with tunnels are shown using beachballs with P-axes as red dipoles; (d) The inferred model of the probability of strainbursting realisation (of different intensity Σd_{SB}) is plotted as functions of modelled extreme depth of failure, d_f^e. The data used for model fit is shown using symbols**

5 Assessment of displacement and energy demand imposed on ground support

The DBSD methodology proposed by Kaiser & Moss (2022) includes the following key components[2], illustrated in schematic diagram in Figure 8:

- Ground support's displacement capacity is consumed as it is deformed after support installation.
- Dynamic demand has both energy and displacement components.
- Excavation damage may not necessarily be attributed to high-energy demand. The scenarios of gradual consumption of support capacity (e.g. due to multiple episodes of stress fracturing and rock bulking behind the wall) and dynamic loading with significant displacement and relatively minor energy are also possible and need to be assessed.

As discussed in this paper, seismic data can be used to track and forecast the demand imposed on ground support.

Firstly, seismic data can help to assess the consumption of support capacity (branch AB of the demand path in Figure 8). The cumulative effect of the past episodes of dynamic stress fracturing can be tracked using the approach presented in Section 4. The inferred cumulative depth of strainbursting multiplied by bulking factor, BF[3], provides an estimate of translation along the horizontal axis in Figure 8. The possibility of gradual bulking of stress fracturing rock (not accompanied by the radiation of detectable seismic waves) also needs to be taken into account when assessing the translation from A to B in Figure 8.

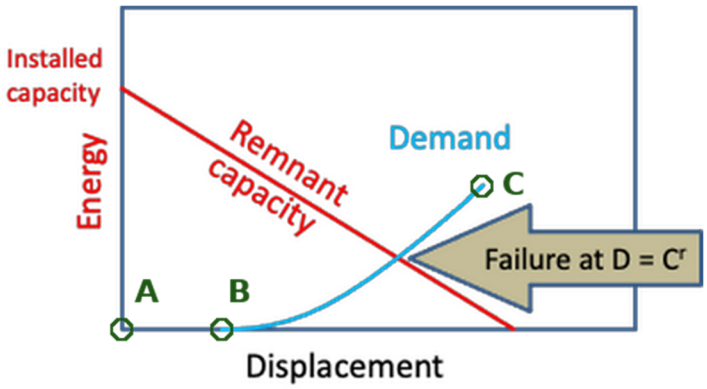

Figure 8 Schematic displacement versus support capacity chart with support failure when the displacement and energy demand (blue) reach the remnant support capacity (red). The labelled points A, B and C are discussed in the text. The figure is modified from Kaiser & Malovichko (2022)

Another utilisation of seismic data is related to the branch BC of the demand path. There are two aspects of it:

1. Forensic analysis of damaging seismic events or large events without damage. It is considered that the branch BC of demand has materialised and the main focus is on comparing it with the remnant capacity ('Failure' in Figure 8). The characteristics of this branch can be established in the following way:
    a. Depth of strainbursting, d_{SB}, is inferred from seismic moment (Section 2) and multiplied by bulking factor, BF, providing an estimate of the displacement demand component (horizontal axis of plot in Figure 8).
    b. Bulking duration, t_B (Section 2) is used in the calculation of bulking velocity, which is translated to kinetic energy (vertical axis of plot in Figure 8).

2 The other components of methodology (e.g. preventive support maintenance) are not listed and discussed here.

3 The bulking factor is not a constant. It depends on support type, pressure and depth of fracturing (Kaiser 2016).

2. Forecast of rockburst hazard, implying that point B represents the current state and branch BC characterises possible dynamic loading which is expected in the future. The seismic data can be used as follows:
    a. The horizontal component of the BC branch (displacement demand) is based on the expected depth of strainbursting and bulking factor. The former can be by evaluated from the extreme depth of failure, $d_f{}^{\mathrm{e}}$, multiplied by parameter q_{SB} as discussed in Section 4.
    b. The vertical component of the BC branch (energy demand) is evaluated using a bulking duration, t_B, characteristic for the mine (i.e. derived from the analysis described in Section 2).
    c. The probability of realisation of the BC branch is established based on the analysis presented in Section 4 (parameter APE_{SB}).

It is noteworthy that the plot shown in Figure 8 can be used in an operational context. This means that such a plot can be constructed for the actual tunnels of a burst-prone mine for given times. The given times may refer to the past (forensic analysis) or future (forecast of rockburst hazard). Different tunnels and parts of tunnels (e.g. back, sidewalls) may have different capacity envelopes (based on the characteristics of the installed ground support system) and different demand paths (depending on the local stress field, rock mass properties, history of seismicity).

6 Conclusion

The current practice of assessing the dynamic loading imposed on ground support of tunnels in case of damaging seismic events is typically focused on the intensity of ground motion (peak ground velocity [PGV] or peak particle velocity [PPV]). Maps of PGV/PPV are often produced based on the source parameters of a large event (location, magnitude); however, the obtained values are not always large enough to explain the damage. Therefore, significant amplification on the surface of the tunnel is sometimes hypothesised[4]. Measurements of amplification and dynamic 1D modelling of relative displacement of supported ground and host rock do not justify using the large values of the amplification factor (Cuello et al. 2017; Malovichko & Kaiser 2020).

The intensity of ground motion may not be useful when analysing strainbursting damage (for which seismic waves are not the cause of damage but rather a byproduct of it and the associated convergence of rock mass around the excavation). It is suggested that assessment of the dynamic demand in terms of the amount and rate of stress fracturing around the tunnels (for example, using depth of strainbursting d_{SB} or bulking velocity $v_B = BF\, d_{SB}/t_B$) be undertaken.

Therefore, the following steps are suggested for completion when damaging seismic events are analysed:

1. Create two maps: a shake map (contours of PGV or PPV) and seismic depth of failure map (contours of d_{SB}). These will characterise two aspects of dynamic loading. The first is relevant for shakedown damage and the second for strainbursting.
2. Quantify the displacement and energy demand for locations with and without damage, and compare these with the remnant support capacity. This can be done by making plots similar to that shown in Figure 8.

The approaches presented in the paper have limitations and further work is required to improve the assessment of demand:

- The calculations of bulking duration (Section 2) and mapping of cumulative depth of strainbursting (Section 3) rely on a particular model of spatio-temporal evolution of stress fracturing around a tunnel, which assumes: (a) a cosine shape of distribution of strainbursting depth along the tunnel,

4 The author came across the examples of using amplification factor of more than 10 to 'explain' the damage by calculated PGV/PPV.

and (b) stress fracturing starts and ends at the centre (location of maximum d_{SB}). Alternative variants of spatio-temporal evolution are also possible (Rigby 2022 2023), e.g. stress fracturing can start at one part of the tunnel and propagate along it to the other part. These models will yield different values of t_B and maps of Σd_{SB}.

- It will be useful to compare the depth of strainbursting inferred from seismic data d_{SB} with the observations (difference between the depth of failure in test holes before and after the crush-type seismic event, which is unfortunately rarely measured).
- The evaluation of bulking duration, t_B, using seismic data is based on the number of assumptions (mechanical coupling of stress fracturing rock with the surrounding rock mass and a particular model of spatio-temporal evolution of stress fracturing). It will be beneficial to compare seismic estimates with the high-sampling (multi-kHz) measurements done by load cells and extensometers installed in the tunnels where dynamic stress fracturing is expected to happen in future.

Acknowledgement

A significant portion of the presented results are based on collaborative work with Peter Kaiser and Alex Rigby. Discussions with Aleksander Mendecki are highly appreciated.

The author is thankful to the mines which provided permission to use their data, and to the anonymous reviewers whose comments/suggestions helped improve and clarify this manuscript.

References

Baker, JW 2015, 'Efficient analytical fragility function fitting using dynamic structural analysis', *Earthquake Spectra*, vol. 31, no. 1, pp. 579–599.

Bird, JF & Bommer, JJ 2004, 'Earthquake losses due to ground failure', *Engineering Geology*, vol. 75, pp. 147–179.

Boatwright, J 1980, 'A spectral theory for circular seismic sources; simple estimates of source dimension, dynamic stress drop, and radiated seismic energy, *Bulletin of the Seismological Society of America,* vol. 70, no. 1, pp. 1–27.

Brune, JN 1970, 'Tectonic stress and the spectra of seismic shear waves from earthquakes', *Journal of Geophysical Research*, vol. 75, no. 26, pp. 4997–5009.

Brune, JN, Archuleta, RJ & Hartzell, S 1979, 'Far-field S-spectra, corner frequencies, and pulse shapes', *Journal of Geophysical Research,* vol. 84, no. B5, pp. 2262–2272.

Cuello, D, Mendecki, A & Mountfort, PJ 2017, 'Ground motion amplification at the skin of excavations', in JA Vallejos (ed.), *Proceedings of the 9th International Symposium on Rockbursts and Seismicity in Mines*, Society for Mining, Metallurgy & Exploration, Engelwood, pp. 216–220.

Dziewonski, AM & Woodhouse, JH 1983, 'An experiment in systematic study of global seismicity: Centroid-moment tensor solutions for 201 moderate and large earthquakes of 1981', *Journal of Geophysical Research,* vol. 88, no. B4, pp. 3247–3271.

Hasegawa, H, Wetmiller, R & Gendzwill, D 1989, 'Induced seismicity in mines in Canada—an overview', *Pure and Applied Geophysics,* vol. 129, no. 3/4, pp. 423–453.

Julia, J, Nyblade, AA, Durrheim, R, Linzer, L, Gok, R, Dirks, P & Walter, W 2009, 'Source mechanisms of mine-related seismicity, Savuka mine, South Africa', *Bulletin of the Seismological Society of America*, vol. 99, no. 5, pp. J2801–2814.

Kaiser, P, McCreath, D & Tannant, D 1996, *Canadian Rockburst Support Handbook*, Geomechanics Research Centre, Sudbury.

Kaiser, PK 2016, 'Ground support for constructability of deep underground excavations – Challenges of managing highly stressed ground in civil and mining projects', *Sir Muir Wood Lecture of International Tunnelling Association at World Tunnelling Congress*, Longrine, Avignon.

Kaiser, P & Moss, A 2022, 'Deformation-based support design for highly stressed ground with a focus on rockburst damage mitigation', *Journal of Rock Mechanics and Geotechnical Engineering,* vol. 14, issue 1, pp. 50–66.

Kaiser, PK & Malovichko, DA 2022, 'Energy and displacement demands imposed on rock support by strainburst damage mechanisms', in M Diederichs (ed.), *Proceedings of the 10th International Symposium on Rockbursts and Seismicity in Mines*, Society for Mining, Metallurgy & Exploration, Englewood.

Kostrov, BV & Das, S 1988, *Principles of Earthquake Source Mechanics*, Cambridge University Press, Cambridge.

Madariaga, R 1976, 'Dynamics of expanding circular fault', *Bulletin of the Seismological Society of America*, vol. 66, no. 3, pp. 639–666.

Malovichko, D & Kaiser, PK 2020, 'Dynamic model for seismic shakedown analysis', *Proceedings of the 54th US Rock Mechanics/Geomechanics Symposium*, American Rock Mechanics Association, Alexandria.

Malovichko, DA 2022, 'Utility of seismic source mechanisms in mining', *Proceedings of the Tenth International Symposium on Rockbursts and Seismicity in Mines*, Society for Mining, Metallurgy & Exploration, Englewood.

Malovichko, DA & Rigby, A 2022, 'Description of seismic sources in underground mines: dynamic stress fracturing around tunnels and strainbursting', *arXiv preprint*.

McGarr, A 1991, 'Observations constraining near-source ground motion estimated from locally recorded seismograms', *Journal of Geophysical Research*, vol. 96, no. B10, pp. 16495–16508.

McGarr, A 1992, 'Moment tensors of ten Witwatersrand tremors', *Pure and Applied Geophysics*, vol. 139, no. 3/4, pp. 781–800.

Mendecki, AJ 2016, *Mine Seismology Reference Book: Seismic Hazard*, Institute of Mine Seismology, Kingston.

Morissette, P & Hadjigeorgiou, J 2019, 'Ground support design for dynamic loading conditions: a quantitative data-driven approach based on rockburst case studies', *Journal of Rock Mechanics and Geotechnical Engineering*, vol. 11, pp. 909–919.

Potvin, Y & Wesseloo, J 2013, 'Towards an understanding of dynamic demand on ground support', in Y Potvin & B Brady (eds), *Ground Support 2013: Proceedings of the Seventh International Symposium on Ground Support in Mining and Underground Construction*, Australian Centre for Geomechanics, Perth, pp. 287–304, https://doi.org/10.36487/ACG_rep/1304_18_Potvin

Rigby, A 2022, *Higher-degree Moment Tensor Inversion*, report.

Rigby, A 2023, 'Dynamic modelling of strainbursting around tunnels', in J Wesseloo (ed.), *Ground Support 2023: Proceedings of the 10th International Conference on Ground Support in Mining*, Australian Centre for Geomechanics, Perth, pp. 151–164.

Ryder, JA 1988, 'Excess shear stress in the assessment of geologically hazardous situations', *Journal of the Southern African Institute of Mining and Metallurgy*, vol. 88, no. 1, pp. 27–39.

Silver, PG 1983, 'Retrieval of source-extent parameters and the interpretation of corner frequency', *Bulletin of the Seismological Society of America,* vol. 73, no. 6, pp. 1499–1511.

Somerville, P, Irikura, K, Graves, R, Sawada, S, Wald, D, Abrahamson, N, … & Kowada, A 1999, 'Characterizing crustal earthquake slip models for the prediction of strong ground motion', *Seismological Research Letters*, vol. 70, no. 1, pp. 59–80.

Stickney, MC & Sprenke, KF 1993, 'Seismic events with implosional focal mechanisms in the Coeur d'Alene Mining District, northern Idaho', *Journal of Geophysical Research*, vol. 98, no. B4, pp. 6523–6528.